IUST
Iran University of Science and Technology

Iranian Journal of Electrical and Electronic Engineering

Journal Homepage: ijeee.iust.ac.ir

Modeling and simulation of piezoelectric-based train-induced vibration energy harvester railway track monitoring system

Shuvojit Kundu *, Tuhel Ahmed* and Jia Uddin**(C.A.)

Abstract: This study aims to evaluate a cantilever beam type piezoelectric energy harvester operating on train-induced vibrations for powering Wireless Sensor Networks (WSNs) used in railway track monitoring systems. Harvester's behaviors under different conditions are simulated in MATLAB using the analytical model. Natural frequency, maximum deflection, and stress are calculated with greater precision using eigen frequency and stationary analysis using COMSOL Multiphysics. At a base excitation of 2 g and a resonant frequency of 4.38 Hz, the simulated results showed that the developed energy harvester prototype could generate up to 14 V of AC output voltage and 550 mW of output power. These findings highlight the promising potential of the proposed energy harvester for transforming train mechanical energy into electrical power. This energy harvester's viability and dependability for real-world applications in monitoring railway tracks are supported by developed analytical and simulation models.

Keywords: COMSOL Multiphysics, Energy harvester, Train-induced vibration, Railway track monitoring.

1 Introduction

WITH advancements in the Internet of Things (IoT), energy harvesting, and wireless sensor technology have led to the development and deployment of autonomous systems in various applications. These include health monitoring of civil structures, fault identification in industrial machines, automation of living and working environments, weather forecasting, aircraft tracking and health monitoring, and monitoring of bridges and railway tracks. . The economy of densely populated nations is wholly reliant on an effective transportation system. The railway is the most essential component of the transportation sector for transporting massive amounts of products and people. For an effective railway transmission system, railway tracks are crucial to the security of transportation. Therefore, a vast railway network is installed in different countries as shown in Table 1.

Railway tracks experience continuous wear and tear from factors like train weight, harsh weather, and dynamic stresses. An effective modern solution is an IoT-based monitoring system for railway tracks, which can provide real-time data and insights to address these issues. An IoT based railway track monitoring system is shown in Figure 1. There are multiple wireless sensor nodes (WSNs) positioned above the rail line that gather data from the rail line and send it to the gateway sensor node via wireless data transmission modules. The data is communicated to the user through the gateway sensor unit.

Iranian Journal of Electrical & Electronic Engineering, 2025.
Paper first received 11 May 2024 and accepted 22 Sep 2024.
* Shuvojit Kundu, Information & Communication Engineering, Hannam University, Daejeon, South Korea
E-mail: theshuvojit@gmail.com, a.tuhel71@gmail.com
** Jia Uddin, AI and Big Data Department, Endicott College, Woosong University, Daejeon, South Korea.
E-mails: jia.uddin@wsu.ac.kr
Corresponding Author: Jia Uddin.

Table 1. List of railway networks installed in different countries/territory [26].

Countries	Installed Railway Track(km)
United States	220,480
China	150,000
Russia	105,000
India	92,952
Canada	49,422
Germany	40,625
Argentina	36,966
Australia	33,168
Brazil	29,817
France	29,273

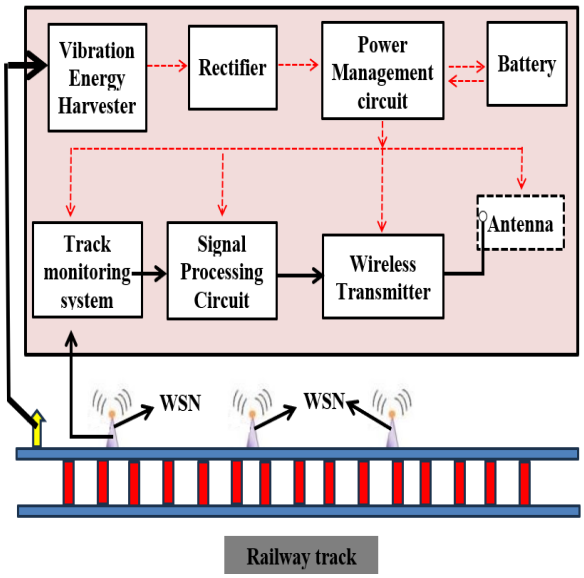

Fig. 1 IoT based self powered railway track monitoring system.

A significant challenge for Wireless Sensor Networks (WSNs) used in railway track monitoring is providing a reliable power source. Typically, these WSNs rely on batteries, which have a limited lifespan and require frequent maintenance such as replacement or recharging.[1] Given the extensive and often inaccessible locations of many WSNs along railway tracks, maintaining these batteries is impractical. To ensure continuous operation, a long-lasting alternative power source is essential. Energy harvesters offer a viable solution by replacing batteries, as they can continuously convert ambient energy sources into useful electrical power. Table 2 illustrates the various ambient energy sources available around railroad tracks.

Several methods exist for transforming the energy contained in these forms into usable electrical power.

Table 2. Different ambient energy sources [2].

Energy sources	Power density μW/cm^2
RF energy	0.0002-1
Vibration Energy	200
Airflow	177
Solar (outdoor)	7500
Thermal energy	60
Temperature variation	10
Acoustic energy	191

Most of these energy sources have limitations. The efficiency of wind power plants varies widely depending on topography and climate. Sound and radio waves have a low output power density, making them unsuitable for use as a primary energy source on a large scale. Similarly, the density of solar energy is greatest in dry, cloudless regions and lowest in sunny ones. The vibrational energy of the railway, on the other hand, is a viable alternative. Using an electromagnetic or piezoelectric transduction mechanism, vibration energy in the railway track can be harnessed and used.

Researchers have investigated using train-induced vibrations to power WSNs for railway monitoring. For instance, Perez et al. developed a tram-mounted electromagnetic energy harvester with two degrees of freedom. [3]. The vibration energy harvester is merely a permanent magnet and coils. Numerical simulation and actual data suggest that the energy harvester can output 6.5 mW. The inductive voice coil system invented in [4] turns the vertical deflection of a track into electrical power. As the track deflected, a voltage was generated in the coil that was attached to the rail and traveled vertically through the stationary magnetic field. The average power with a 7.5 kΩ load resister was calculated to be 0.16 mW in the simulation. Many distinct designs of piezoelectric train induced vibration energy harvester systems have been created to accommodate a wide range of potential installation sites. Cantilever types, stacked types, bilateral fixed types, and circular types are the most common line-side structures for piezoelectric energy harvesters [5].

In a railway setting, piezoelectric vibration energy harvester based on a cantilever mechanism are the simplest method for harvesting vibration energy. To capture the vibrational energy from passing trains on a bridge, Cahill et al. designed a piezoelectric energy harvester based on a cantilever beam [6]. The estimated frequency of the bridge's energy harvesting is shown to be consistent with the tested natural frequency, and the

maximum output voltage was found to be 99 mV. Gao et al. aimed to create a prototype to supply electricity to out-lying areas [7]. A detailed modeling and simulation of a railway track-mounted electromagnetic energy harvester are presented. Li et al. investigated the performance of piezoelectric Vibration energy harvester's-based cantilevers when subjected to varying resistors and frequencies [8]. The power output of a piezoelectric harvester is optimized at its resonance point. Wang et al. investigated the efficiency of a piezoelectric stack device coupled to train tracks for energy harvesting. Their findings suggest that this piezoelectric energy harvesting technology could effectively power wireless sensors in railway systems. [9]. Hou et al. proposed installing a piezoelectric vibration energy harvester based on a layered structure atop the rail transit bridge [10]. Based on simulation results, the max output voltage and current can be as high as 195.8 V and 5.6 mA, respectively, for a total of 1.09 W. The examined piezoelectric energy harvester has a power density of up to 0.048 mW/cm3, which is double that of current low-frequency piezoelectric vibration energy harvesters. Cantilever-structured piezoelectric vibration energy harvester use on railway piezoelectric energy harvesters were proposed by Pasquale et al. [11].

The proposed energy harvester's performance was evaluated using a miniature train bogie. The results demonstrate that at its maximum capacity, the harvester can produce an output power of 4.12 mW. A piezoelectric vibration energy harvester based on a cantilever construction was studied by Song et al. [12] and put on a superconducting Maglev train. Experimental results showed that the harvester's output voltage rose with increasing vibration frequency, reaching a maximum of over 6 V.

This work involves modeling and simulating a train-induced vibration-based cantilever beam-type piezoelectric energy harvester using MATLAB and COMSOL Multiphysics. The energy generated by this harvester can power Wireless Sensor Networks (WSNs) in railway track monitoring systems. Unlike previous designs that relied on electromagnetic transduction, this developed piezoelectric energy harvester uses piezoelectric technology. There is no analytical modeling for optimization of different parameters. However, in this work an analytical model and simulation is presented for piezoelectric energy harvester to optimize the device working parameters. Stationary and eigenfrequency analyses are conducted on the harvester to estimate the maximum deflection and stress in the beam, considering the device's dimensions and the amplitude of applied vibrations.

2 Analytical Modeling of Piezoelectric Energy Harvester

Figure 2 depicts the architecture of the rail track-induced vibration piezoelectric energy harvester. A Unimorph cantilever piezoelectric plate is designed to make the device. The device is supposed to be tightly fixed to the railway track or the body of the rail car. A proof mass is attached at the free end of the beam to lower the natural frequency of the piezoelectric structure. When the train is passing, it induces vibration in the body as well as in the track. The piezoelectric beam vibrates due to the vibration of the rail car. According to the piezoelectric effect, When the beam vibrates under the influence of external sources, voltage is generated across its terminals. This voltage is used to charge the backup power bank for further usage. For small amplitudes of applied vibration, deflection is produced in the piezoelectric beam, which produces electrical energy according to the piezoelectric principle. Piezoelectric basic equations are [6]:

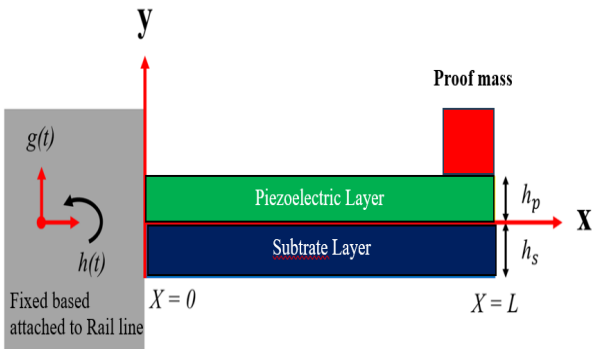

Fig. 2 Architecture of train-induced vibration piezoelectric energy harvester.

$$D = e\epsilon + E\epsilon^T \tag{1}$$

$$\sigma = C\epsilon + eE \tag{2}$$

where e is the strain, D is the electrical displacement, C is the stiffness, E is the Electrical field, σ is the stress, ϵ is the PZT stress constant, ϵ^T is the permittivity. For piezoelectric harvester, the governing equation is:

$$\begin{bmatrix} D1 \\ D2 \\ D3 \end{bmatrix} = \begin{bmatrix} 0 & 0 & 0 & 0 & e_{15} & 0 \\ 0 & 0 & 0 & e_{24} & 0 & 0 \\ e_{31} & e_{32} & e_{33} & 0 & 0 & 0 \end{bmatrix} \begin{bmatrix} \varepsilon_1 \\ \varepsilon_2 \\ \varepsilon_3 \\ \tau_{23} \\ \tau_{31} \\ \tau_{12} \end{bmatrix} + \begin{bmatrix} \varepsilon_{11}^T & 0 & 0 \\ 0 & \varepsilon_{22}^T & 0 \\ 0 & 0 & \varepsilon_{33}^T \end{bmatrix} \begin{bmatrix} E_1 \\ E_2 \\ E_3 \end{bmatrix} \tag{3}$$

The strain of the layer can be considered in one direction, and the strain in the other two directions can be assumed to be zero because the thickness of a piezoelectric layer in a piezoelectric based harvester is often considerably lower than the length and width. That's why we can reduce the complexity of the constitutive Equation (3).

$$D_3 = e_{31}\varepsilon_1 + \varepsilon_{33}^T E_3 \tag{4}$$

After reducing the complexity of the constitutive Eq. (3) we got the Eq. (4).

The stiffness of a cantilevered beam multilayered can be written as:

$$K_{beam} = \frac{3b}{L^3}\left(\sum_{i=1}^{n_1} n_{i\,E_i} h_i^3 + \sum_{j=1}^{n_2} n_{j\,E_j} h_j^3\right) \tag{5}$$

where b is the beam width, n_1 is the number of piezoelectric layers, n_2 is the number of electrode layers, E_i and E_j are young moduli, h_i is the height of each piezoelectric layer, h_j is the height of each electrode layer. Since, the beam is Unimorph, only a single layer of piezoelectric material and substrate material will be used. Equation 5 becomes as:

$$K_{beam} = \frac{b}{4L^3}(E_i h_i^3 + E_j h_j^3) \tag{6}$$

Multilayered cantilever beams that have a mass at their tip can have their effective mass calculated as:

$$m_{eff} = m_T + 0.23bL\left(\sum_{i=1}^{n_1} n_{i\,\rho_i h_i} + \sum_{j=1}^{n_2} n_{j\,\rho_j h_j}\right) \tag{7}$$

where ρ_j and ρ_i denote the densities of the electrode and piezoelectric materials and m_T is the tip mass. For the Unimorph cantilever beam, equation (7) can be modified as:

$$m_{eff} = m_T + 0.23bL(\rho_i h_i + \rho_j h_j) \tag{8}$$

From equation (8), the corresponding natural frequency of the cantilevered beam can be derived as:

$$\omega_{beam} = \sqrt{\frac{K_{beam}}{m_{eff}}} \tag{9}$$

When a vibrating beam is subjected to a bending moment M(x), the average effective stress per unit length is:

$$\sigma_{Beam} = \frac{1}{L}\int_0^L \frac{M(x)C}{I}\ \mathrm{dx} \tag{10}$$

Cantilever beam length (L), maximum displacement (C), moment of inertia (I), and orientation (x) along the beam's length (x) are all inputs into the following equation. The moment $M(x)$, when the beam to be in resonance can be evaluated as:

$$M(x) = k_{Beam}.Y.X \tag{11}$$

where Y denotes the tip deflection or vibration amplitude and is evaluated as:

$$Y = \frac{1}{2\zeta}\left(\frac{m_{\,eff}*a}{k_{eff}}\right) = \frac{1}{2\zeta}\left(\frac{a}{\omega_t^2}\right) \tag{12}$$

here ζ is the damping ratio and is evaluated using the co-relationship.

$$\zeta = \frac{1}{2\pi} ln\left(\frac{a_1}{a_2}\right) \tag{13}$$

where a_1 and a_2 are consecutive amplitudes of the beam. Putting the values of tip deflection in equation 11, the moment $M(x)$ will become:

$$M(x) = k_{Beam}.\frac{1}{2\zeta}\left(\frac{a}{\omega_t^2}\right).X \tag{14}$$

Substituting equation 14 in equation10, the maximum stress in the beam will become:

$$\sigma_{Beam} = \frac{1}{L}\int_0^L \frac{k_{Beam}.\frac{1}{2\zeta}\left(\frac{a}{\omega_t^2}\right).XC}{I}\ \mathrm{dx} \tag{15}$$

Integrating the equation (15) along the length of the beam, the equation for stress will be modified as:

$$\sigma_{Beam} = \frac{1}{L}\frac{m_{eff}.a.C}{2\zeta I}\int_0^L x\ \mathrm{dx} = \frac{m_{eff}.a.C.L}{4.\zeta.I} \tag{16}$$

The voltage generated is directly proportional to the average effective stress in the cantilevered beam, due to the piezoelectric nature of the material and the electrodes extending along the length of the beam.

$$V = \frac{-d_{31}*t_p*\sigma_{beam}}{\varepsilon} \tag{17}$$

where t_p is the thickness of the piezoelectric layer, $-d_{31}$ is the strain constant of the piezoelectric material, and is the dielectric constant. Integrating equations 16 with 17, the voltage equation will become:

$$V = \frac{-d_{31} * t_p * m_{eff.a.C.L}}{4.\zeta.I.\varepsilon} \quad (18)$$

The output power of cantilever beam based piezoelectric vibrational energy is given as:

$$P = \frac{V^2 * R_L}{(R_S + R_L)^2} \quad (19)$$

where R_L is the load resistance and R_s is the piezoelectric cantilever beam impedance (also called source resistance). The source resistance depends on the frequency ω of the beam as [25]:

$$R_s = \frac{1}{\omega_t * C_p} \quad (20)$$

when $R_L = R_s$ the output power is maximum, this condition is called impedance matching. the corresponding power in this case is given as:

$$P = \frac{V^2}{4 * R_s} \quad (21)$$

2.1 Fonts

3 COMSOL modeling and simulation

COMSOL Multiphysics is a robust software for simulating and modeling diverse engineering challenges. In this study, a piezoelectric energy harvester with a cubical mass, designed to harness train-induced vibrations, is modeled and analyzed. The FEM technique in COMSOL Multiphysics is employed to evaluate the maximum deflection at the tip of the piezoelectric beam and to determine the mode shapes at various natural frequencies in response to applied vibrations. The process of modeling and simulating a circular plate piezoelectric energy harvester using COMSOL Multiphysics are illustrated in Figure 3 and are discussed in the following subsections.

3.1 Creating Geometry

In the realm of energy harvesting, optimized geometry plays a crucial role. It is important to remember that the harvester's high-power density is only available at the low natural frequency. The proposed device geometry is shown in Figure 4. It consists of a piezoelectric layer and a rectangular substrate layer. The precise geometrical specifications of the proposed device are displayed in Table 3.

3.2 Adding material

PZT-5A is employed for the piezoelectric component, whereas brass is used for both the substrate layer and the proof mass. The suggested device's dimensions and material properties are shown in Table 3.

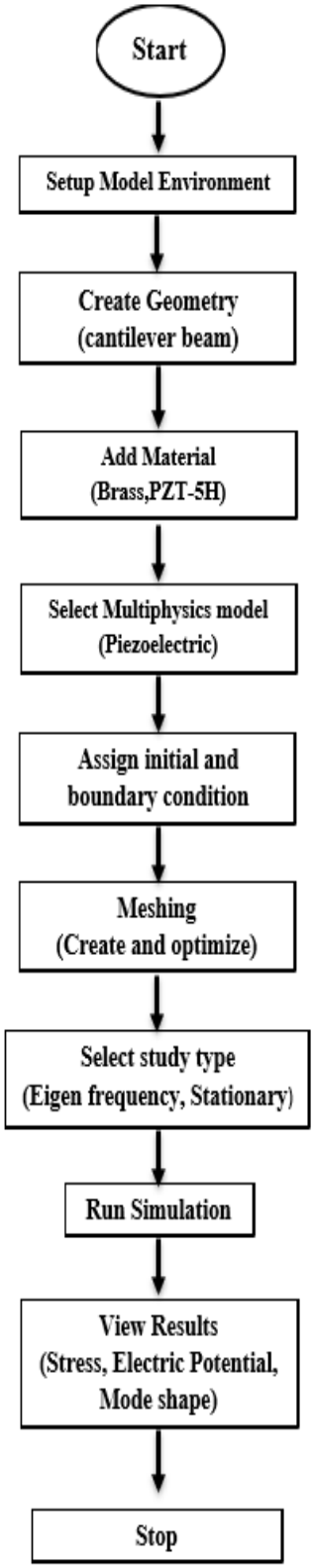

Fig. 3 Steps in COMSOL

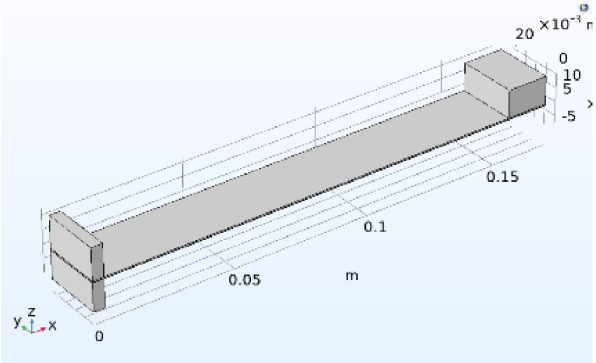

Fig. 4 Steps in COMSOL

Table 3. Material and variable description.

Description	Variable	Values	Unit
Elastic layer Length	L_e	171	mm
PZT layer Length	L_p	171	mm
Elastic layer Width	We	22	mm
PZT layer Width	Wp	22	mm
Thickness of PZT layer	h_p	0.052	mm
Thickness of the elastic layer	H_e	0.012	mm
Volume of proof mass	V	15x15x10	Mm^3
Density of proof mass	ρ_m	8,587	Kg/m^3
Elastic layer elasticity	Y_e	97	Gpa
PZT layer elasticity	Y_p	66	Gpa
Elastic layer density	P_e	8785	Kg/m^3
PZT layer density	ρ_p	7800	Kg/m^3
Piezoelectric Charge	d31	$1.75x10^{-9}$	C/N

3.3 Adding Multiphysics

In this study, piezoelectric Multiphysics is assigned to the device, which is comprised of electrostatics and solid mechanics physics. The physics of solid mechanics is based on the equations of Navier and yields results such as stresses, strains, and dis-placements.

3.4 Initial and boundary condition

The device is modeled with all areas free to move, except for the fixed end of the beam, which is firmly attached to the rail line for stability. Linear elastic properties such as Young's modulus, density, and Poisson's ratio, are assigned values from the material library.

3.5 Creating Mesh

Figure 5 illustrates a mesh geometry. COMSOL Multiphysics has numerous meshing defaults. This simulation uses tetrahedral mesh. The domain is small, hence an exceptionally normal element size is used. Meshing yielded 18672 boundary elements, 43967 domain elements, and 844 edge elements.

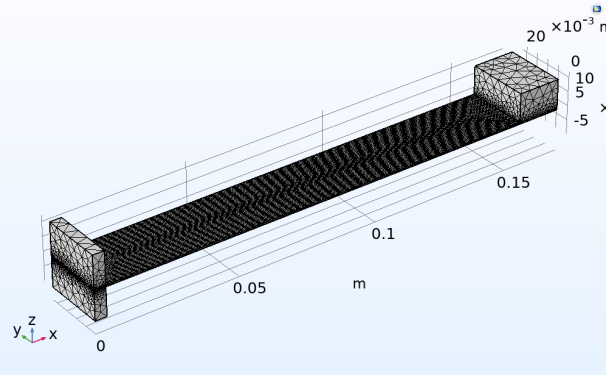

Fig. 5 Mesh result.

3.6 Adding Analysis

Various analyses have been conducted to assess how different parameters impact the performance of piezoelectric energy harvesters. There are two types of analyses used in this investigation: stationary analysis and Eigen frequency analysis. Displacement at rest can be calculated by stationary analysis. The first six of the proposed device's natural frequencies and the mode shapes they produce can be found with the help of eigenfrequency analysis.

4 Citations and References

When vibration is applied to the fixed support of the beam, it causes deflection, with the maximum deflection occurring at the free end and the minimum at the fixed end, as illustrated in Figure 6. Piezoelectric beams bend and twist, causing tensions within the plates themselves. The vibration given to the device causes a corresponding fluctuation in stress. Figure 7 displays the simulation results showing that at 5 m/s acceleration, the greatest stress created is 2.87 MPa at The fixed end of the beam is securely attached, while the minimum stress developed is 0.001360 MPa, occurring at the free end of the beam.

The eigen frequencies and mode shapes are the outputs of an eigen frequency analysis. Finding the six lowest eigen frequencies (natural frequencies) and the geometry of the associated modes is the goal of the eigen frequency analysis, as illustrated in Table 4.

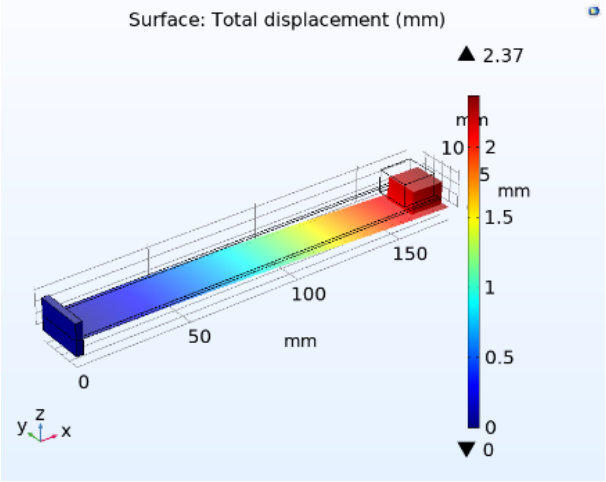

Fig. 6 Maximum deflection observed in the device.

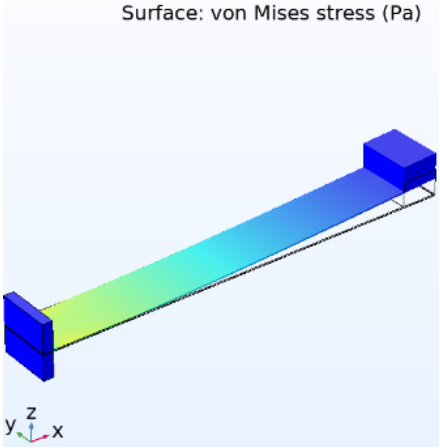

Fig. 7 Maximum stress produced in the device.

MATLAB simulation is used to analyze the different factors based on the analytical model developed in the previous section. There is a strong correlation between the length, width, and thickness of a cantilever beam and its stiffness, as shown in Figure 8. Stiffness values decline noticeably from 18 N/m to 8 N/m as the length of the cantilever beam grows from 150 mm to 200 mm (Figure 8(a)). This finding is consistent with the general rule that beams with a greater length are less rigid because they bend more easily under the same strain. In contrast, beams that are shorter are stronger and less likely to deform under load. Figure 8(b) shows the relationship between beam width and stiffness of the beam. The rigidity of a cantilever beam increases dramatically from 6 N/m to 17 N/m as its width grows from 10 mm to 30 mm. Figure 8(c) and 8(d) demonstrate that, when the thickness of the layer is increased, it increases the stiffness of the beam. When the thickness of the substrate layer varies from 100 µm to 300 µm, the stiffness of the beam increased from 12.9 N/m to 15.7 N/m. Similarly, when the thickness of the PZT layer is changed from 400 µm to 1000 µm, the beam stiffness varies from 5 N/m to 72 N/m. From these results, the stiffness is more affected by changes in the thickness of the PZT layer compared to the substrate layer.

Table 4. Eigen frequencies and modes shapes of device.

Frequency (Hz)	Mode	Mode Shape
4.56	1	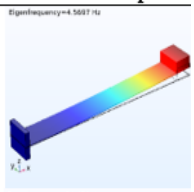
54.48	2	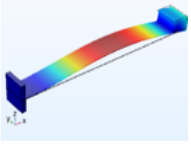
61.132	3	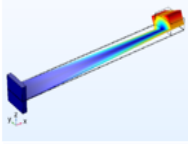
156.68	4	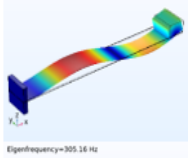
305.16	5	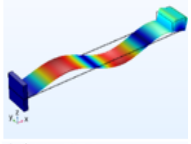
407.99	6	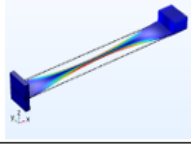

The dependency of the beam's natural frequency on beam dimension is depicted in Figure 9. The dynamic behavior of a cantilever beam is best understood by Figure 9(a) displaying the relationship between the length of the beam and its natural frequency at constant beam width and thickness. A significant drop in natural frequency is shown as beam length is increased from 150 mm to 200 mm, with values going from 7.1 Hz to 1.2 Hz.

This trend can be attributed to the fundamental principle that longer beams exhibit lower natural

frequencies, indicating greater flexibility and a longer period for oscillation. However, shorter beams indicate stiffer materials with faster oscillation cycles due to their higher inherent frequencies. Certainly, the width and thickness of each layer affect the natural frequency of a cantilever beam in addition to its length.

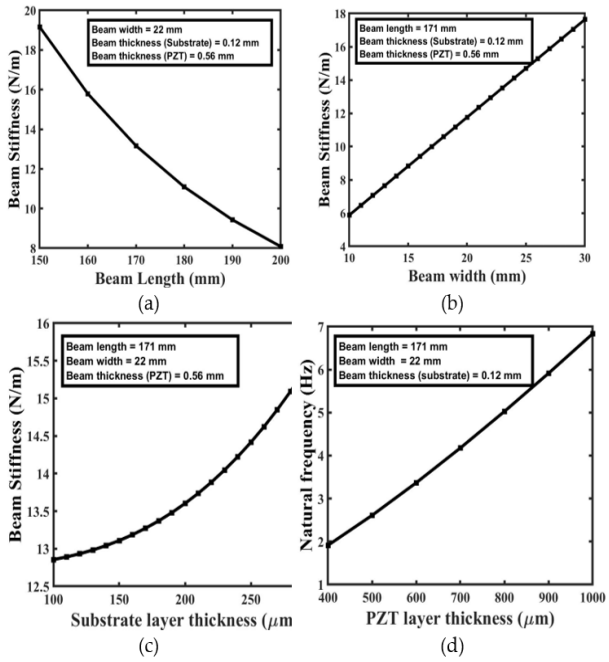

Fig. 8 Beam stiffness with (a) length of the beam, (b) width of the beam, (c) substrate layer thickness, (d) PZT layer thickness.

When the length and thickness are held constant, the relationship between natural frequency and beam width is shown in Figure 9(b). The beam's natural frequency falls as its width increases. Beam natural frequency with substrate layer thick-ness for a fixed beam size is analyzed in Figure 9(c). The natural frequency rises dramatically as the thickness of the substrate layer rises. Figure 9(d) depicts the linear relationship between the natural frequency of a beam and the thickness of a PZT layer for a beam of constant length and width. Increases in PZT layer thickness result in a higher natural frequency.

Figure 10 depicts the relationship between the cantilever beam's tip mass and natural frequency. By adding a proof mass at the free end of the beam, the natural frequency is drastically reduced. As the proof mass varies between 0 g to 300 g, the frequency decreases from 4.4 Hz to 1 Hz. This decrease in natural frequency is directly attributable to the additional mass, which effectively modifies the beam's inertia and stiffness, resulting in a decreased oscillation rate. In numerous applications, such as vibration isolation, energy harvesting, and precision sensing, modulating the natural frequency to meet specific requirements is essential for optimal performance.

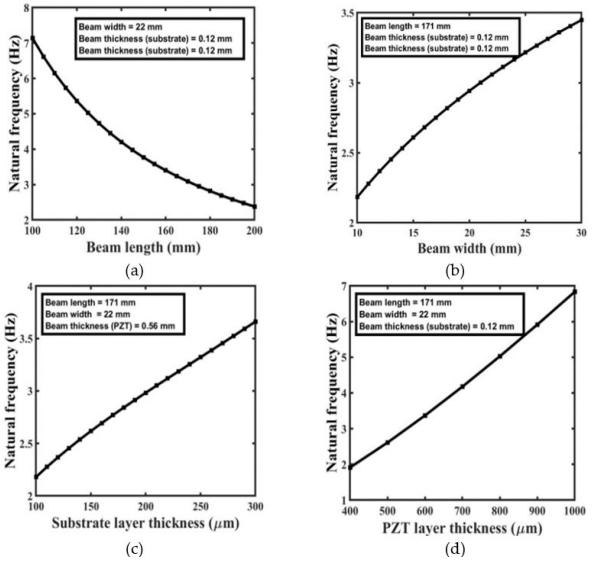

Fig. 9 Beam natural frequency versus: (a) length of the beam, (b) width of the beam, (c) substrate layer thickness, (d) PZT layer thickness.

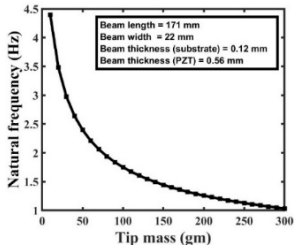

Fig. 10 Natural frequency vs. tip mass.

When a cantilever beam piezoelectric energy harvester is excited at its base, the stress generated within the beam is highly dependent on its dimensions (length, width, and layer thickness) as depicted in Figure 11. Maximum stress increases with beam length because longer beams bend and deform more under an applied excitation. In contrast, the maximum stress decreases as beam width increases because broader beams provide greater resistance to bending, hence reducing the stress concentration. Increasing the beam's length from 150 mm to 200 mm results in a corresponding increase in maximum stress from 2.8 MPa to 3.9 MPa.

The maximum stress in a cantilever beam as a function of tip mass is shown in Fig. 12. The tension in the beam varies significantly as the tip mass is changed from 0 gm to 300 gm, going from 1.8 MPa to 10 MPa. This finding demonstrates how the increased mass at the beam's top has a dramatic effect on the beam's structural behaviors and stress distribution. Higher stresses in the beam are a

direct result of the increased forces and deformations caused by the heavier load at the top.

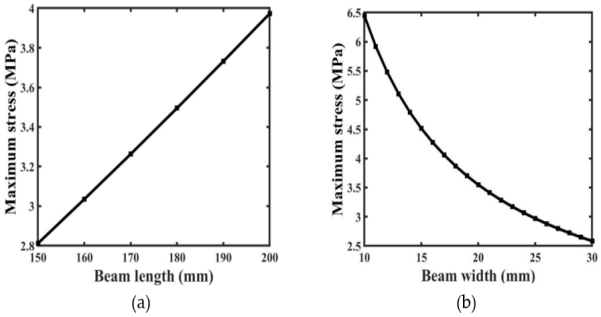

Fig. 11 Maximum stress versus (a) beam length (b) beam width.

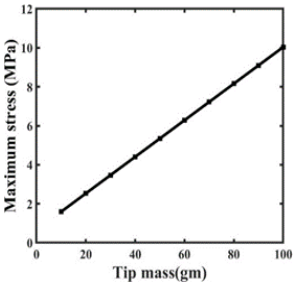

Fig. 12 Maximum stress versus tip mass.

When a cantilever beam piezoelectric energy harvester is excited at its base, the input acceleration has a significant effect on the stress within the beam as depicted in Figure 13. The maximum stress in the beam dramatically shifts from 0.5 MPa to 6.8 MPa as the input acceleration is doubled from 1 g to 2 g.

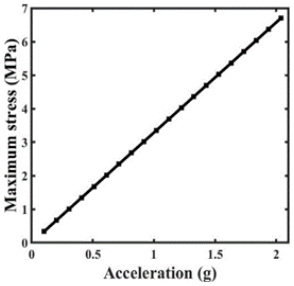

Fig. 13 Maximum stress versus acceleration.

Figure 14 illustrates the relationship between the output voltage produced by the piezoelectric energy harvester and the variation in beam length. The harvester's output voltage varies from 6.3 V to 8.8 V as the beam's length is changed from 150 mm to 200 mm. The maximum output voltage of the harvester is 7.3 V when the beam length is 171 mm, the beam width is 22 mm, and the input acceleration is 1 g. There is an inverse relationship between output voltage and beam width as shown in Figure 14(b).

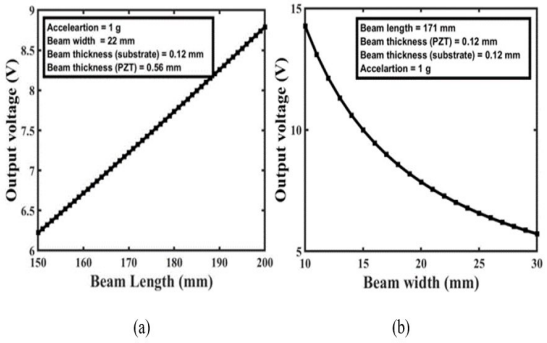

Fig. 14 Output voltage versus. (a) beam length, (b) beam width.

Figure 15 depicts the relationship between the output voltage generated by the piezoelectric energy harvester and the variation in input base acceleration. Depending on the magnitude of the applied base acceleration, the harvester's output voltage might vary widely. When the input acceleration is increased from 1 g to 2 g, the harvester's output voltage varies dramatically, going from 0.5 V to 15 V.

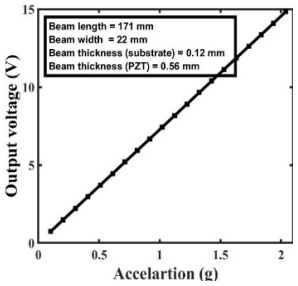

Fig. 15 Output voltage versus acceleration.

Power output by the piezoelectric beam-type energy harvester as a function of input resistance is shown in Figure 16. The input base acceleration has a considerable effect on the output power. As the input base acceleration is doubled from 1 g to 2 g, the harvester's output power ranges from 100 μW to 55 mW, demonstrating a significant boost in its ability to generate electricity. The highest output power of the harvester is 13 mW, and it is achieved under specified conditions with a beam length of 171 mm, width of 22 mm, thickness of 68 mm, and under an input acceleration of 1 g.

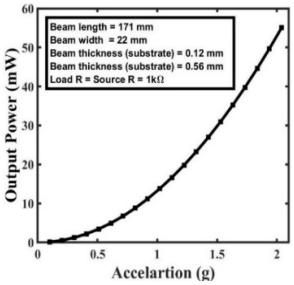

Fig. 16 Output power versus load resistance.

5 Comparison and Discussion

The performance of the train-induced vibration energy harvester prototypes that have been produced is compared with the performance of train-induced vibration type harvesters that had been developed in the past. Table 5 shows all the train-induced vibration energy harvester types that have been recorded. These comparisons are carried out concerning the place where the installation was carried out, the internal resistance, the frequency, the output-input base acceleration, the output voltage, and the output power. When compared to piezoelectric harvesters, the electromagnetically developed harvesters have a comparatively lower internal impedance. Piezoelectric energy harvesters, on the other hand, have a high impedance.

The voltage production of the developed prototypes is quite better than the developed energy harvester that has ever been reported. However, when evaluated based on power output, the prototypes generated in this work can generate higher output power than all the reported energy harvesters combined. It is evident from this comparison that the energy harvester that was produced in this work can produce higher voltage and output power than most of the reported harvesters that have been developed in the past.

Table 5. Eigen frequencies and modes shapes of device.

Type	Installation position	Frequency (Hz)	Input acceleration (g)	Load resistance (Ω)	Voltage (V)	Power (mW)	Ref.
Electromagnetic	Line side	6	-	44.6	2.23	119	[7]
	Onboard	8	-	-	2.5	100	[13]
	Line side	7-500	2	-	-	45.5	[14]
	Line side	27	-	-	1.7	10	[15]
	Onboard	28	0.8	-	-	6.5	[3]
	Onboard	-	-	300	7.07	28.4	[16]
	Line side	4	-	50	-	196	[17]
	Onboard	-	-	-	-	263	[18]
Piezoelectric	Line side	-	0.2	44	1.8	-	[19]
	Line side	50	0.21	15000	-	1.843	[20]
	Onboard	26	-	11000	-	3	[21]
	Line side	-	-	55024	-	1.03	[22]
	Onboard	-	1	-		0.3	[23]
	Line side	16.6	-	-	0.144	-	[6]
	Line side	1.8		-		1.09	[10]
	Line side	3-6	-	40000	-	40	[24]
This prototype	Line side	4.56	2	100	14.8	550	This work

6 Conclusion

This study aimed to evaluate the cantilever beam-type energy harvester that operates on train-induced vibrations and the developed prototypes may be used to sup-ply power for wireless sensor setworks employed in the condition monitoring of railway networks. The study covered a detailed discussion of the architecture, working mechanism, modeling, and simulation of the proposed energy harvester. An analytical model was built to estimate several factors, some of which include maximal stress, stiffness, natural frequency, output voltage, and output power. Different factors were examined employing MATLAB simulations based on the analytical model, yielding important insights into the harvester's performance under changing situations. COMSOL Multiphysics modeling and simulation of the proposed energy harvester device was carried out to validate the analytical modeling and acquire more accurate findings. The natural frequency, maximum deflection, and stress of the device were determined through eigenfrequency and stationary analysis. Simulation results indicated that the prototype energy harvester could produce up to 14 V of AC voltage and 550 mW of output power when subjected to a base excitation of 2 g and a resonant frequency of 4.38 Hz. These findings show that the suggested energy harvester has great potential as a means of transforming mechanical energy from trains into electrical power. The analytical and simulation models that were developed and validated show that the suggested energy harvester is practical and reliable for use in monitoring railway tracks in the real world.

Funding

This research is funded by Woosong University Academic Research 2024.

References

[1] Roundy S. J. “Energy Scavenging for Wireless Sensor Nodes with a Focus on Vibration to Electricity Conversion,” University of California, Berkeley, 2003.

[2] Khan F. U. and Ahmad S., “Flow type electromagnetic based energy harvester for pipeline health monitoring system,” Energy Convers. Manag., vol. 200, no. June, pp. 112089, 2019, doi: 10.1016/j.enconman.2019.112089.

[3] Perez, M., Chesne, S., Jean-Mistral, C., Billon, K., Bouvet, S., and Clerc, C., “A two degree-of-freedom electromagnetic vibration energy harvester for the railway infrastructure monitoring,” Smart materials, adaptive structures and intelligent systems, pp. 1-5, 2018.

[4] Ghasemi-Nejhad M. N., Pourghodrat A., Nelson C.

A., Phillips K. J., and Fateh M., "Improving an energy harvesting device for railroad safety applications," In: Active and Passive Smart Structures and Integrated Systems, vol. 7977, pp. 297-305, 2011.

[5] Wang P., Wang Y. F., Gao M. Y., and Wang Y., "Energy harvesting of track-borne transducers by train-induced wind," J. Vibroengineering, vol. 19, no. 3, pp. 1624–1640, 2017, doi: 10.21595/jve.2017.17592.

[6] Cahill P., Hazra, B., Karoumi, R., Mathewson, A., and Pakrashi V., "Data of piezoelectric vibration energy harvesting of a bridge undergoing vibration testing and train passage," Data in brief, vol. 17, pp. 261-266, 2018.

[7] Gao M. Y., Ping W., Yong C., Rong C., and Cheng L., "A rail-borne piezoelectric transducer for energy harvesting of railway vibration," Journal of vibroengineering, vol. 18, no. 7, pp. 4647-4663, 2016.

[8] Li J., Jang S., and Tang, J., "Design of a Bimorph Piezoelectric Energy Harvester for Railway Monitoring," J. Korean Soc. Nondestruct. Test., vol. 32, no. 6, pp. 661–668, 2012, doi: 10.7779/jksnt.2012.32.6.661.

[9] Wang J., Shi Z., Xiang H., and Song, G., "Modeling on energy harvesting from a railway system using piezoelectric transducers," Smart Materials and Structures, vol. 24, no. 10, pp.105017, 2015.

[10] Hou W., Zheng Y., Guo W., and Pengcheng G., "Piezoelectric vibration energy harvesting for rail transit bridge with steel-spring floating slab track system," Journal of Cleaner Production, vol. 291, pp. 125283, 2021.

[11] De Pasquale G., Soma A., and Fraccarollo F., "Piezoelectric energy harvesting for autonomous sensors network on safety-improved railway vehicles," In: Proceedings of the Institution of Mechanical Engineers, Part C: Journal of Mechanical Engineering Science, vol. 226, no. 4, pp. 1107–1117, doi: 1177/095440621141."

[12] Song D., Jang H., Kim S.B., and Sung T.H., "Piezoelectric energy harvesting system for the vertical vibration of superconducting Maglev train," J. Electroceram., vol. 31, pp. 35–41, doi: 10.1007/s10832-013-9817-9."

[13] De Pasquale G., Somà A., and Fraccarollo F., "Piezoelectric energy harvesting for autonomous sensors network on safety-improved railway vehicles," In: Proceedings of the Institution of Mechanical Engineers, Part C: Journal of Mechanical Engin., vol. 226, no. 4, pp. 1107-1117, 2012.

[14] Gao M., Li Y., Lu J., Wang Y., Wang P., and Wang L., "Condition monitoring of urban rail transit by local energy harvesting," International Journal of Distributed Sensor Networks, vol. 14, no. 11, pp. 1550147718814469, 2018.

[15] Hosseinkhani A., Younesian D., Eghbali P., Moayedizadeh A., and Fassih A., "Sound and vibration energy harvesting for railway applications: A review on linear and nonlinear techniques," Energy Reports, vol. 7, pp. 852-874, 2021.

[16] Lin T., Wang J. J., and Zuo L., "Efficient electromagnetic energy harvester for railroad transportation," Mechatronics, vol. 53, pp. 277-286, 2018.

[17] Pan Y., Lin T., Qian F., Liu C., Yu J., Zuo J., and Zuo L. "Modeling and field-test of a compact electromagnetic energy harvester for railroad transportation," Applied Energy, vol. 247, pp. 309-321, 2019.

[18] Wang Y., Wang P., Li S., Gao M., Ouyang, H., He, Q., and Wang, P. "An electromagnetic vibration energy harvester using a magnet-array-based vibration-to-rotation conversion mechanism," Energy Conversion and Management, vol. 253, pp. 115146, 2022.

[19] Song Y. "Finite-element implementation of piezoelectric energy harvesting system from vibrations of railway bridge," Journal of Energy Engineering, vol. 145, no. 2, pp. 04018076, 2019.

[20] Hou W., Li Y., Guo W., Li J., Chen Y., and Duan X., "Railway vehicle induced vibration energy harvesting and saving of rail transit segmental prefabricated and assembling bridges," Journal of Cleaner Production, vol. 182, pp. 946-959, 2018.

[21] Mouapi A., "Design, Modeling and Simulation of Piezoelectric Microgenerator for application in Underground Vehicles," IEEE International Conference on Environment and Electrical Engineering and IEEE Industrial and Commercial Power Systems Europe (EEEIC / I&CPS Europe), Genova, Italy, 2019, pp. 1-5, doi: 10.1109/EEEIC.2019.8783737.

[22] Li S., Wang Y., Yang M., Sun Y., Wu F., Dai J., Wang P., and Gao M. "Investigation on a broadband magnetic levitation energy harvester for railway scenarios," Journal of intelligent material systems and structures, vol. 33, no. 5, pp. 653-668, 2022.

[23] Wischke M., Masur M., Kröner M., and Woias P., "Vibration harvesting in traffic tunnels to power wireless sensor nodes," Smart Materials and Structures, vol. 20, no. 8, pp. 085014, 2011.

[24] Costanzo L., Lo Schiavo A., Sarracino A., and

Vitelli M., “Stochastic Thermodynamics of an Electromagnetic Energy Harvester,” Entropy, vol. 24, no. 9, pp. 1222, 2022.

[25] " Charless K.Alexander,Matthew N.O, and Sadiku, Fundamentals of Electric Circuits. 6th Edition, 2018.

[26] Largest railway network in the world - check top 10 list (no date) Testbook. Available at: https://testbook.com/static-gk/largest-railway-network-in-the-world (Accessed: 11 May 2024).

Shuvojit Kundu is a master’s student in the Department of Information and Communication Engineering at Hannam University, Daejeon, Republic of Korea. Alongside his master’s studies, he is currently working as an Assistant Research Engineer at Dongyoung Industry Co., Ltd, Republic of Korea. He obtained his B.Sc. in Railway Engineering from Woosong University, Daejeon, Republic of Korea in 2021. His research interests encompass IoT, renewable energy, and modern power systems. He can be contacted at email: theshuvojit@gmail.com

Tuhel Ahmed is a master’s student in the Department of Information and Communication Engineering at Hannam University, Daejeon, Republic of Korea. He holds a B.Sc. in Railway Engineering from Woosong University (2021). Throughout his academic journey, he has engaged in diverse projects, including the development of railway airbrake systems and real-time monitoring systems involving 3D modeling and IoT. His research interests encompass machine learning and AI technology applied to modern power systems. He can be contacted at email: a.tuhel71@gmail.com

Jia Uddin is as an Assistant Professor, Department of AI and Big Data, Endicott College, Woosong University, Daejeon, South Korea. He received Ph.D. in Computer Engineering from University of Ulsan, South Korea, M.Sc. in Electrical Engineering (Specialization: Telecommunications), Blekinge Institute of Technology, Sweden, and B.Sc. in Computer and Communication Engineering, International Islamic University Chittagong, Bangladesh. He was a visiting faculty at School of computing, Staffordshire University, United Kingdom. He was an Associate Professor in Department of Computer Science and Engineering, Brac University, Dhaka, Bangladesh. His research interests are Industrial Fault Diagnosis, Machine Learning/Deep Learning based prediction and detection using multimedia signals. Information and Communication Engineering at Hannam University, Daejeon, Republic of Korea. Alongside his master’s studies, he is currently working as an Assistant Research Engineer at Dongyoung Industry Co., Ltd, Republic of Korea. He obtained his B.Sc. in Railway Engineering from Woosong University, Daejeon, Republic of Korea in 2021. His research interests encompass IoT, renewable energy, and modern power systems. He can be contacted at email: jia.uddin@wsu.ac.kr